**Jian Zhou**[1, 2], **Jun Wang**[1*], **Honggang Bu**[3]

# Fabric Defect Detection Using a Hybrid and Complementary Fractal Feature Vector and FCM-based Novelty Detector

**DOI:** 10.5604/01.3001.0010.5370

[1] **Ministry of Education, Key Laboratory of Textile Science & Technology Donghua University,**
Shanghai, 201620, China
* E-mail: junwang@dku.edu.cn

[2] **Ministry of Education, Jiangnan University, Key Laboratory of Eco-textiles,**
Wuxi, Jiangsu 214122, China

[3] **North Valley Aircraft,**
11647 33rd St SE, Valley City, ND, 58072, USA

**Abstract**
*Automated detect detection in woven fabrics for quality control is still a challenging novelty detection problem. This work presents five novel fractal features based on the box-counting dimension to address the novelty detection of fabric defect. Making use of the formation of woven fabric, the fractal features are extracted in a one-dimension series obtained by projecting a fabric image along the warp and weft directions, where their complementarity in discriminating defects is taken into account. Furthermore a new novelty detector based on fuzzy c-means (FCM) is devised to deal with one-class classification of the features extracted. Finally, by jointly applying the features proposed and the FCM based novelty detector, we evaluate the method proposed for eight datasets with different defects and textures, where satisfying results are achieved with a low overall missing detection rate.*

**Key words:** *defect detection, box-counting dimension, fuzzy c-means, novelty detection.*

## Introduction

In modern weaving mills, performing a visual examination of fabric products is a standard process before reaching customers, as defects can severely affect products' visual quality. Currently visual inspection is still manually performed by well-trained human inspectors, a job whose efficiency is greatly limited by the human inspector's experience. For this reason, the automation of fabric inspection based on computer vision and emerging artificial intelligence techniques have drawn considerable attention, and numerous approaches have been proposed to address this issue in recent decades [1].

Generally images of normal fabrics are dominated by the texture, which always exhibits high periodicity among sub-patterns. If there is a defect occurring in a fabric, the local regularity (periodicity) of the fabric will be disrupted, causing a local anomaly against its homogeneous texture background. Such anomalies always manifest in various ways, e.g. local structure or intensity change. Basically how to find versatile features that can robustly describe normal textures while sensitive to such anomalies (defects) is the basis for designing detection algorithms. Typical features used include the parameters of the textured model [2-3], features based on the grey-level co-occurrence matrix [4], Fourier features [5], multi-scale wavelet decomposition coefficients [6-7], and Gabor filtering features [8]. With little taking into account of the complementarity of the features extracted, the aforementioned features or simple group of them generally result in performing well for certain types of fabric or defects and poorly for others.

Associated with texture roughness, the use of fractal based features such as the fractal dimension is another important approach for texture analysis. Fractal-based texture analysis was introduced by Pentland [9] in 1984, whose experimental results showed that there was a high positive correlation between texture roughness and fractal dimension, i.e. the rougher the texture, the larger the fractal dimension, with similar results found in [10-11]. Since the fractal dimension offers a decent measurement for the roughness of a texture surface, it is intuitive to use the fractal dimension as the feature for discriminating between a normal fabric texture and defective texture. Typical works include the following: Conci and Proença utilised the differential box-counting dimension for fabric defect detection [12], and Wen adopted another fractal feature, namely the Hurst coefficient, for identifying defects [13]. It is noted that the fractal features used in [12-13] are too few and simple, and only one fractal feature is used, which usually leads to a high false detection rate, e.g. up to 28% [12]. In fact, the single fractal feature, especially the fractal dimension, has a drawback in characterising local details of the texture, which might possess an identical or quite close fractal dimension for different textures. Some researchers were aware of the limitation of using a single feature, and different fractal-based features were proposed in order to achieve better results. For example, Bu and Huang extracted four box-counting dimensions calculated from different measuring scale ranges [14]. In addition, the use of multi-fractals or feature combination can be seen in other applications [15-16].

In this paper, we introduce five new fractal features for fabric defect detection. The features proposed integrate local and globe texture information, which is able to describe the inherence of the fabric texture deeply. There are two distinctive differences between the fractal features proposed and previous features: (1) the features proposed make use of the woven fabric's horizontal and vertical details in projection operations; (2) the complementarity of the features extracted are taken into consideration in order to capture local and global details of the fabric texture. Besides this, all fractal features are extracted in a one-dimension series, rather than in two-dimension images. Considering fabric defect detection belongs to the category of one-classification or novelty detection problems, this paper also devises a new novelty detector based on fuzzy c-means clustering to handle the one-class or novelty classification of features extracted.

The rest of this paper is organised as follows: a brief introduction to the box-counting dimension and fuzzy c-means is firstly presented. The methodology appears in the next section, and the following is the experimental results and discussion. Conclusions are in the last section.



Zhou J, Wang J, Bu H. Fabric Defect Detection Using a Hybrid and Complementary Fractal Feature Vector and FCM-based Novelty Detector.
*FIBRES & TEXTILES in Eastern Europe* 2017; 25, 6(126): 46-52. **DOI:** 10.5604/01.3001.0010.5370

## Background

### Box-counting dimension

In fractal geometry, there are many methods that can be used to define the fractal dimension, such as the box-counting dimension (or box dimension), Hausdorff dimension and correlation dimension etc. In this work, the box-counting dimension, also known as the Minkowski dimension, is used to calculate the fractal dimension of a fabric image, as it can deal with non-self-similar fractals and be simply implemented with a computer. The key idea of the box-counting dimension is about covering with boxes, i.e. to count how many boxes are required to cover a set in different scales, Suppose that $N(\delta)$ is the number of boxes of side length $\delta$ required to cover a set $S$, the box-counting dimension is defined as:

$$D(S) = \lim_{\delta \to 0} \frac{\log N(\delta)}{\log(1/\delta)}. \quad (1)$$

Here the box dimensions are based on one-dimension sequences, and an example of a one-dimension curve is presented to demonstrate the procedures of calculating the box dimension. Let us denote the curve as $S(x), x = 1, 2, \ldots, M$ and $N(\delta)$ is the minimal number of $\delta \times \delta$ squares needed to cover $S(x)$. According to ***Equation (1)***, there is $\log(N(\delta)) \propto D(S)\log(1/\delta)$, and the $D(S)$ can be estimated by the slope of the linear portion of $\log(N(\delta))$ against $\log(1/\delta)$. Specifically let $T$ be any sub-sequences of length $\delta$ in $S(x)$, and then the minimal number of $\delta \times \delta$ squares needed to cover $S(x)$ is given by,

$$n(\delta) = \mathrm{Int}\left[\frac{\max(T) - \min(T)}{\delta}\right] + 1, \quad (2)$$

where, Int[] is the integer rounding operator, and max($T$) and min($T$) are the largest and smallest values in the sequence $T$, respectively. Then $N(\delta)$ can be obtained by calculating the mean of every sub-sequence in $T$ with ***Equation (2)***, which is given by,

$$N(\delta) = \frac{E(n(\delta)) \times M}{\delta}, \quad (3)$$

where, $E()$ is the expectation operator. Having obtained a different $N(\delta)$ by changing the value of $\delta$, the slope of the linear portion of $\log(N(\delta))$ against $\log(1/\delta)$ can be estimated by means of fitting those points in the least-squares sense. ***Figure 1*** depicts the fitting result of a data sequence of length 32 with $\delta = 2, 3, 4, 5, 6$, and the fitting equation is $y = 1.28x + 5.33$, i.e. the box dimension $D(S)$ is 1.28.

***Figure 1.*** *Fitting result for calculating box dimension.*

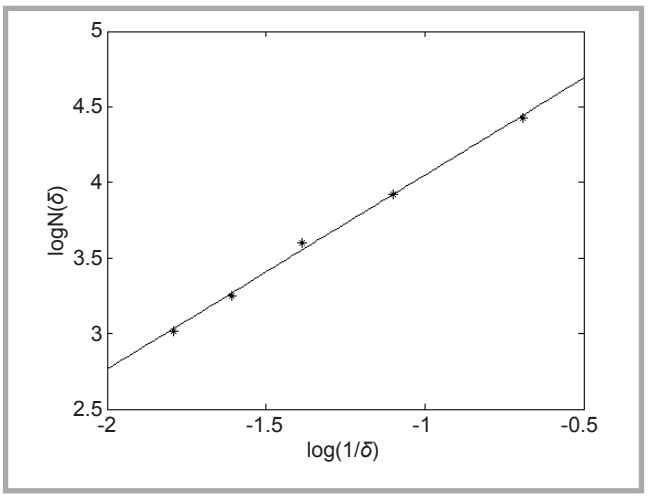


### Fuzzy c-means model

In machine learning, cluster analysis or clustering is one of the most important unsupervised learning methods of partitioning a set of unlabelled data into different groups according to a certain similarity. Different from supervised methods, the clustering techniques do not need any prior knowledge of the labels of data, potentially allowing to reveal the underlying structures within data. The clustering methods can be loosely classified into two categories: hard and soft clustering. In hard clustering, the data is grouped into hard-assigned clusters, where each data point completely belongs to one cluster, e.g. a k-means clustering algorithm. Rather than make a hard decision for each data point, soft clustering allows a data element to belong to more than one cluster, where the soft decision is made according to their degrees of belonging (quantified by the membership function). One of the most commonly used soft clustering is the fuzzy c-means (FCM) algorithm [17], which has been successfully applied to many applications, such as image segmentation [18] and fault diagnosis [19].

Given a set of interest $\{x_i\}_{1 \le i \le N}$, the FCM algorithm attempts to partition the data set into $C$ different groups with cluster centres $\{c_j\}_{1 \le j \le C}$. Thus the objective function $J_m$ for finding those centres is defined as:

$$J_m = \sum_{i=1}^{N}\sum_{j=1}^{C} u_{ij}^m \left\| x_i - c_j \right\|_2^2, \ 1 \le m < \infty \quad (4)$$

where, $u_{ij}$ is the degree of belonging of $x_i$ to the cluster $j$, and $m \ge 1$ is the weight controlling the degree of fuzziness. Since the cluster centres $c_j$ and degrees of belonging $u_{ij}$ can be represented by each other through the necessary conditions for minimising $J_m$, the alternating optimisation strategy can be used to minimise ***Equation (4)***. The implementation is composed of the following procedures:

S1: Given $C$ and $m$, initialise $c_j^{(0)}$ with random numbers;

S2: For $t = 0, 1, \ldots, n$, update $u_{ij}$ and $c_j$ using the following formula:

S3: Update $u_{ij}$: $u_{ij}^{(t)} = \dfrac{\left(\left\| x_i - c_j^{(t)} \right\|_2^2\right)^{\frac{2}{m-1}}}{\sum_{k=1}^{C}\left(\left\| x_i - c_k^{(t)} \right\|_2^2\right)^{\frac{2}{m-1}}}$

S4: Update $c_j$: $c_j^{(t+1)} = \dfrac{\sum_{i=1}^{N}(u_{ij}^{(t)})^m x_i}{\sum_{i=1}^{N}(u_{ij}^{(t)})^m}$

S5: Repeat steps S3 and S4 until $\|U^{(t+1)} - U^{(t)}\|_F < \varepsilon$ is achieved, where $U = [u_{ij}]$ is the membership matrix.

## Methodology

### Fractal feature extraction

Due to the fact that most real-world image textures do not exhibit stringent self-similarity, instead an approximate or statistical self-similarity, the fractal dimension calculated by the box-counting method does not possess the quality of scale invariance, which was also pointed out by Pruess [20], namely that limited observation resolution made the estimated box dimension vary with box scales. In our preliminary experiments, we noted that there was a positive association between the box dimension and box scales. Thus in order to alleviate the drawback of instability in estimating the box dimension with a fixed box scale, this work attempts to calculate the box dimension in a range of box scales, meanwhile addressing the

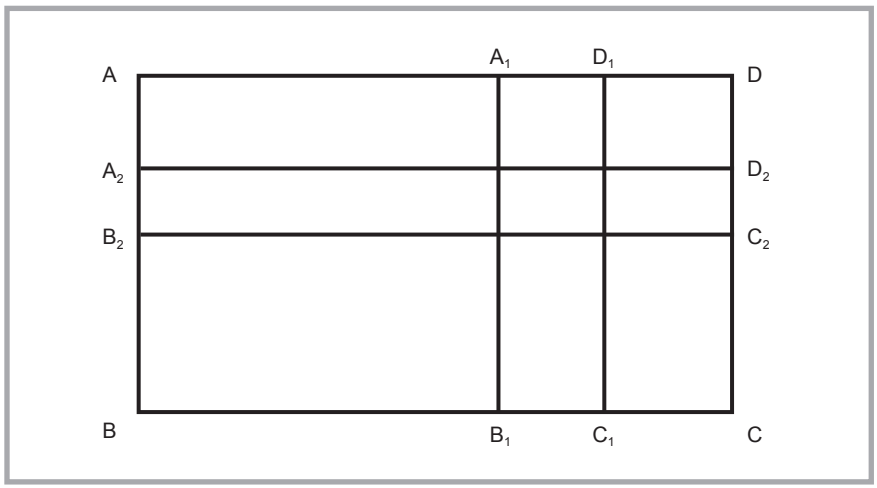


***Figure 2.*** *Illustration of feature extraction.*

complementariness of the fractal features extracted. Moreover all the features proposed are extracted in one-dimension sequences by taking advantage of the formation of the fabric (interlaced with two mutually perpendicular yarn systems).

Without loss of generality, we illustrate the feature extraction scheme with a rectangle window ABCD, which is illustrated in ***Figure 2***. Let us denote an image patch of size $L_1 \times L_2$ (AB × AD) as W, a sub-window $A_1B_1C_1D_1$ of size $P_1 \times L_2$ as $W_1$, and a sub-window $A_2B_2C_2D_2$ of size $L_1 \times P_2$ as $W_2$. With the definition, the box dimension features are extracted based on W, given as follows:

- **Fractal feature 1:** Perform projection operation along AD and AB, i.e. compute the mean grey-level values along AD and AB, and denote the resultant two sequences as $S_v$ and $S_h$ with a length of $L_1$ and $L_2$, respectively, combine $S_v$ and $S_h$ into a new sequence with a total length of $L_1 + L_2$, and calculate the box dimension of the new sequence using ***Equation (1)***, denoting fractal feature 1 as $D_1$.
- **Fractal features 2 and 3:** For $W_1$, perform a projection operation along $A_1D_1$, i.e. compute the mean grey-level values along $A_1D_1$, calculate the box dimension of the resultant sequence, transverse $W_1$ through the whole window W along the horizontal direction, obtaining $L_1 - P_1 + 1$ box dimensions, and extract the maximum and minimum box dimensions among them, denoting fractal features 2 and 3 as $D_2$ and $D_3$.
- **Fractal features 4 and 5:** For $W_2$, perform a projection operation along the $A_2B_2$ direction, i.e. compute the mean grey-level values along the $A_2B_2$ direction, calculate the box dimension of the resultant sequence, transverse $W_2$ through the whole window W along the vertical direction, obtaining $L_2 - P_2 + 1$ box dimensions, and extract the maximum and minimum box dimension among them, denoting fractal features 4 and 5 as $D_4$ and $D_5$.

Conveniently we combine the five fractal features extracted into a hybrid feature vector $D = [D_1\ D_2\ D_3\ D_4\ D_5]$. In particular, $D_1$ mainly reflects the global information of fabric textures, which is more robust than the other four features, crucial for characterising the texture in most cases; D2~D5 are sensitive to local changes, capable of compensating for $D_1$ in charactering details. Furthermore our preliminary experiments demonstrated that $D_2$ and $D_3$ are particularly sensitive to weft-wise defects, as the local abrupt of weft-wise defects can be well revealed; similarly, $D_4$ and $D_5$ are capable of finding the warp-wise defects. Note that all aforementioned features are calculated in a measuring scale range of 2~6 pixels.

### Feasibility validation of features

In this section, we take two real-world fabric samples as examples to demonstrate the validation of the fractal features proposed. Here we hypothesise about the features from normal and defective samples obeying normal distribution, and the statistical hypothesis test, namely the t-test, is applied to objectively evaluate the effectiveness of the features proposed in differentiating between normal and defective fabric textures. It is notable that the t-test is not only able to judge the significance of the validation of a feature, but can tell the degree of effectiveness of the various features, i.e. the larger a statistic, the more effective and discriminative the power. Suppose that there are two sets of feature samples, $\{x_i\}$ and $\{y_i\}$, calculated from normal and defective samples, and the $T$-statistic to test whether the means of the two groups are statistically different from each other is given by,

$$T = \frac{\mu_1 - \mu_2}{\sqrt{\frac{\sigma_1^2}{n_1} + \frac{\sigma_2^2}{n_2}}} \tag{5}$$

where $\mu_1$ and $\mu$, are the means of samples $\{x_i\}$ and $\{y_i\}$, $\sigma_1^2$ and $\sigma_2^2$ the standard deviation samples $\{x_i\}$ and $\{y_i\}$, and $n_1$ & $n_2$ are the total number of samples $\{x_i\}$ and $\{y_i\}$. Here the $T$-statistic obeys the t-distribution with $n_1 + n_2 - 2$ degrees of freedom and the significance level $\alpha = 0.01$ is used. Thus if $|T| > t_{0.99}$, the feature is considered to be valid (significance).

**Example 1:** ***Figure 3*** presents a typical coarse weft image, where ***Figure 3.a*** is a normal fabric image, ***Figure 3.b*** a defective image, and ***Figure 3.c*** has been divided into 64 patches of size 32 × 32. As shown in ***Figure 3.c***, there are 8 patches containing defects in the last row. The total numbers of normal and defective samples are 64 and 8. Thus the associated statistics are computed as follows: The degree of freedom is equal to 70 (64 + 8 – 2), $t_{0.99} = 2.38$ (one-tailed), and the statistic $|T|$ of the five fractal features $D_1$~$D_5$ are 6.99, 13.59, 10.77, 0.2125 and 8.03. Therefore, in this case, the four features (besides $D_4$) are all valid with a high significance, especially for $D_2$.

**Example 2:** ***Figure 4*** presents a typical double filling image, where ***Figure 4.a*** is a normal fabric, ***Figure 4.b*** a defective image, and ***Figure 4.c*** has been divided into 64 patches of size 32 × 32. As shown in ***Figure 4.c***, there are 8 patches containing defects in the second last column. The total numbers of normal and defective samples are also 64 and 8. Thus the associated statistics are computed as follows: the degree of freedom is equal to 70 (64 + 8 – 2), $t_{0.99} = 2.38$ (one-tailed), and the statistic $|T|$ of the five fractal features $D_1$~$D_5$ are 6.54, 1.84, 5.59, 12.93 and 9.03. Therefore, in this case, the four features (besides $D_2$) are all valid with high significance, especially for feature $D_4$.

As demonstrated above, although the extracted features have different discriminative power for different defect types, the integration of them can ensure that at

least one feature is significant in defect detection practice.

**Construction of novelty detector based on FCM**

As mentioned in the preceding section, fabric defect detection is a kind of novelty detection problem, rendering the conventional FCM model useless for straightforward defect detection, as the FCM is normally used for the data, whose number of clusters is specified. If one tries to cluster normal samples into a centre and cluster the defective samples into several centres with respect to defect types, then one must know whether the input data contain defects or how many defect types there are in it in advance, which is unknown in practice. On the other hand, if the input data do not contain defects, a substantial false detection rate would be achieved, where clustering is conducted on it anyway; even though one tries to cluster the potential defective sample into one centre.

In this paper, we train the FCM with only normal samples, and more than one clustering centre is utilised to describe the stochastic variations of normal samples. For the decision rule, given an unknown sample $y$, if the minimal Euclid distances of $y$ to the clustering centres (obtained after training FCM) exceeds the pre-defined threshold, then $y$ is a defective sample, otherwise a normal one.

**Parameter optimisation:** There are two parameters: the number of clustering centres $C$ and the fuzzy weight $m$. For $C$, a common way is to define a statistic to measure the validity of clustering in order to find the optimum number of clusters. However, a related work remarked that the selection of the number of clusters was a task-specific problem, and it was not justified to use one validity measurement for all the cluster analysis due to the random distribution of data. Compared with different validity measurements, we found that the validity measurement function proposed by Gao was suited to the clustering of normal fabric samples [21]. Given the number of cluster centres $C$, the fuzzy weight $m$ and the total number of training samples $N$, the validity measurement is defined by,

$$FP(C) = \frac{1}{N}\sum_{j=1}^{N}\left(\sum_{i=1}^{C}\mu_{ij}^{m} / \sum_{i=1}^{C}\mu_{ij}\right) - \frac{1}{C}\sum_{i=1}^{C}\left(\sum_{j=1}^{N}\mu_{ij}^{m} / \sum_{j=1}^{N}\mu_{ij}\right) \quad (6)$$

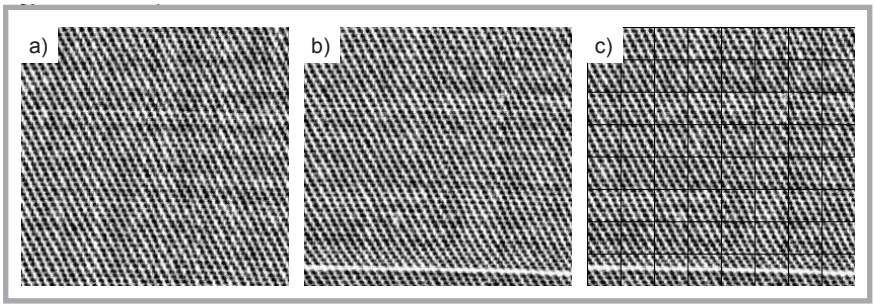


***Figure 3.*** *Fabric image samples: a) normal fabric image, b) defective image, c) illustration of patch division.*

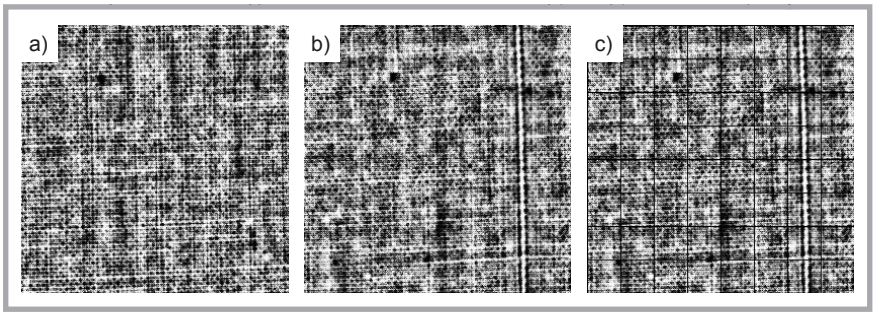


***Figure 4.*** *Fabric image samples: a) normal fabric image, b) defective image, c) illustration of patch division.*

Thus, fixing $m$ and calculating $FP(C)$ with different $C$, the optimum $C$ is the minimum one of set $FP(C)$, where the searching range of $C$ is from 2 to $2ln(N)$ (a commonly used upper boundary).

In terms of $m$, there is no theoretical way of reference, and most researchers choose it empirically or experimentally. For example, Bezdek pointed out that the choice of $m$ was an application specific problem, and suggested a range (1.1 5) for reference [17]; Pal and Bezedek found the range (1.5 2.5) is empirically best for most cases [22]. In this work, our primary experimental results showed that the suitable range of $m$ for normal sample clustering is from 2 to 5. Considering the computing efficiency (a larger $m$ needs less iteration times for the convergence of ***Equation (4)***), here we select m empirically according to the total number of training samples as well, i.e. when the number of training is larger than or equal to 3000, setting $m=4$, otherwise setting $m=2.5$.

## Experiments

To evaluate the efficiency of the fractal features extracted and the FCM novelty detector described in the preceding sections, eight datasets are chosen for testing, including three twill fabrics and five plain fabrics. A detailed configuration of the eight datasets is listed in ***Table 1***, where the samples refer to sub-windows of size $32 \times 32$ pixels. Besides this, necessary pre-processing operations are conducted to obtain comparable features for classification, and histogram equalisation is firstly adopted to help enhance the contrast of defects in the raw fabric images acquired before partitioning into sub-windows. Since the values of raw features vary widely, each fractal feature extracted is normalised to have zero mean unit variance, whose normalised version is given by,

$$x' = \frac{x-\bar{x}}{\sigma}, \quad (7)$$

Where, $\bar{x}$ and $\sigma$ are the mean and standard derivation of $x$.

Having calculated the five normalised fractal features, the FCM classifier proposed needs to be trained with a normal sample in order to find the optimal parameter for practical testing of unknown samples. Here, dataset 1 (see ***Table 1***) is taken as an example to demonstrate the training process:

S1: Choose $m=4$ as the total number of training samples larger than 3000;
S2: Calculate the search range of clusters C: $2 \le C \le 16$ ( $2\ln(4472)=16.8$);
S3: Calculate FP(C) in the range from 2 to 16, which is listed in ***Table 2***.

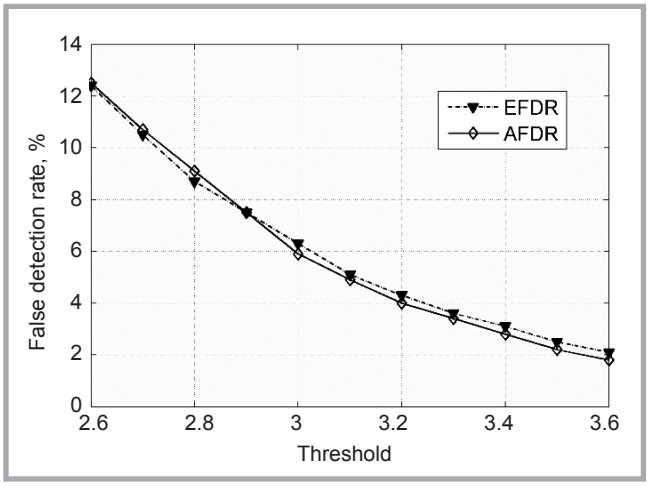


***Figure 5.*** *Trend curves of EFDR and AFDR under varying thresholds.*

From ***Table 2***, it can be seen that $FP(C)$ has the minimum when $C=3$. Thus the optimal clustering numbers for datasets 1 is 3 are (-0.0057, -0.0047, -0.0060, 0.0011, -0.0031), (0.4532, 0.4246, 0.4392, 0.1631, 0.1474) and (-0.4511, -0.4369, -0.4273, -0.1790, -0.1215). Since the features extracted have been normalised with a zero mean, the features from normal samples should fluctuate around zero. That is to say, the first cluster centre is almost located at the origin, and the other two clusterings are symmetrical with respect to the origin. Therefore with the three optimal cluster centres, unknown features will be classified into a defect if any of their distance to the three clusters exceeds the predefined threshold.

Generally the choice of threshold is a non-trivial task due to the absence of negative samples for the estimation of the missing detection rate (MDR). Here we adopt a simple and effective way to determine this parameter, which is to collect an additional sample set from normal samples as the validation set, and conduct a test on it by increasing the threshold with a small step to obtain its false detection rate (FDR) with respect to the threshold used. Then the FDR obtained can be used as an estimated false detection rate (EFDR) in favour of choosing a threshold in practical detection. ***Figure 5*** presents the trend curves of EFDR and the actual false detection rate (AFDR), where EFDR and AFDR are obtained from training samples and testing samples of dataset 1.

As shown in ***Figure 5***, the values of EFDR and AFDR are quite close to each other at a specific threshold, whose trend curves exhibit good agreement under different thresholds. It indicates that EFDR can provide a good prediction for the AFDR, i.e. it is reasonable to use it for the selection of the threshold in practical detection. On the other hand, since the actual MDR is unknown, the threshold selected referring to the EFDR can only make sense in controlling the AFDR in some manner, leaving no clues for actual MDR. Fortunately the FDR and MDR have a negative tendency towards each other, i.e. the larger the FDR, the smaller the MDR. Thus, from the application point of view, if a low MDR is important, it is recommended to choose a threshold with respect to a higher EFDR. Furthermore ***Table 3*** summaries the detection results for all eight datasets.

By examining ***Table 3***, it can be seen that: The number of clusters vary with the datasets, i.e. its optimal are specific to fabric textures. Explicitly the larger the variation of input features, the more clusters are required to describe their loose distribution, i.e. a texture with lower regularity would need more clusters than that of higher regularity. It can be observed from dataset 7 that there are 12 cluster centres for the fabric of low regularity (see ***Table 3***). Moreover twill fabric always needs less centre than plain fabric, as it generally has higher regularity than plain ones.

The average EFDR and AFDR for all datasets are quite close to each other, indicating the robustness of the EFDR in forecasting the AFDR. The reasons for the poor agreement of datasets 4 and 7 are mainly due to the low texture regularity and too few training samples being used.

***Table 1.*** *Sample configuration of the eight datasets.*

| Dataset | Fabric type | Training samples | Testing | |
|---|---|---|---|---|
| | | | Normal samples | Defective samples |
| 1 | Twill | 4472 | 4472 | 302 |
| 2 | Twill | 2960 | 2960 | 84 |
| 3 | Twill | 1792 | 1792 | 256 |
| 4 | Plain | 1820 | 1820 | 170 |
| 5 | Plain | 5010 | 5010 | 320 |
| 6 | Plain | 1608 | 1608 | 216 |
| 7 | Plain | 1168 | 1168 | 101 |
| 8 | Plain | 1474 | 1474 | 76 |

***Table 2.*** *FP(C) for different C.*

| C | 2 | 3 | 4 | 5 | 6 | 7 | 8 | 9 |
|---|---|---|---|---|---|---|---|---|
| *FP* | 0.433 | **-0.934** | 0.078 | -0.229 | -0.786 | -0.134 | -0.387 | -0.190 |
| *C* | 10 | 11 | 12 | 13 | 14 | 15 | 16 | / |
| *FP* | -0.348 | -0.288 | -0.173 | -0.258 | -0.402 | -0.320 | -0.222 | / |

***Table 3.*** *Summary of detection results.*

| Dataset | C | EFDR,% | AFDR,% | MDR,% |
|---|---|---|---|---|
| 1 | 3 | 8.12 | 8.23 | 5.63 |
| 2 | 4 | 2.97 | 3.17 | 1.19 |
| 3 | 3 | 5.64 | 5.64 | 1.56 |
| 4 | 7 | 7.78 | 9.04 | 10.0 |
| 5 | 3 | 4.73 | 4.39 | 5.94 |
| 6 | 5 | 4.98 | 5.29 | 3.24 |
| 7 | 12 | 7.71 | 6.33 | 7.92 |
| 8 | 3 | 6.11 | 5.77 | 2.63 |
| Average | | 6.01 | 5.98 | 4.76 |

Overall the fractal features proposed and the FCM based novelty detector can achieve a 4.76% MDR with a low 5.98% FDR on average. And we also note that those missing detection regions are usually located in the margins or weakness regions of the defects. Undoubtedly the method proposed can successfully label the major regions of defects.

Some figurative examples of detection results are given in ***Figure 6***, where ***Figure 6.a*** and ***6.b*** are the normal and defective images, and ***Figure 6.c*** presents the detection results of ***Figure 6.b***. Note that the red squares represent $32 \times 32$ pixel sub-windows, which are identified as abnormal regions (defects). By viewing ***Figure 6***, it can be found that the features proposed exhibit a good discriminating power on defects of linear shape or structural changes (see the first three columns in ***Figure 6.c***). For the defects in the last column of ***Figure 6.c***, the method proposed is able to detect the majority of defective regions, and the reasons for the missing regions are because they are located at the margins between detecting patches, providing not enough abnormal regions to identify them. Hence, in practical applications, we recommend using smaller patch sizes or overlapping patch division depending on specific process requirements.

## Conslusions

In this work, five fractal features have been extracted in a one-dimension projection series of fabric images by making use of the formation of fabric for defect detection. To better discriminate defects from the normal texture, the complementarity of fractal features extracted are fully taken into account, where the preliminary feasibility of those features in finding defects is verified via the t-test. In feature classification, a new FCM based novelty detector has been constructed to conduct an efficient novelty classification of features extracted, which has shown its effectiveness in handling the random distribution of normal samples. The experimental results for eight fabric datasets show that the method proposed can achieve a 4.76% MDR with a low 5.98% FDR on average, which further confirms the usefulness of the fractal features proposed for the FCM based novelty detector.

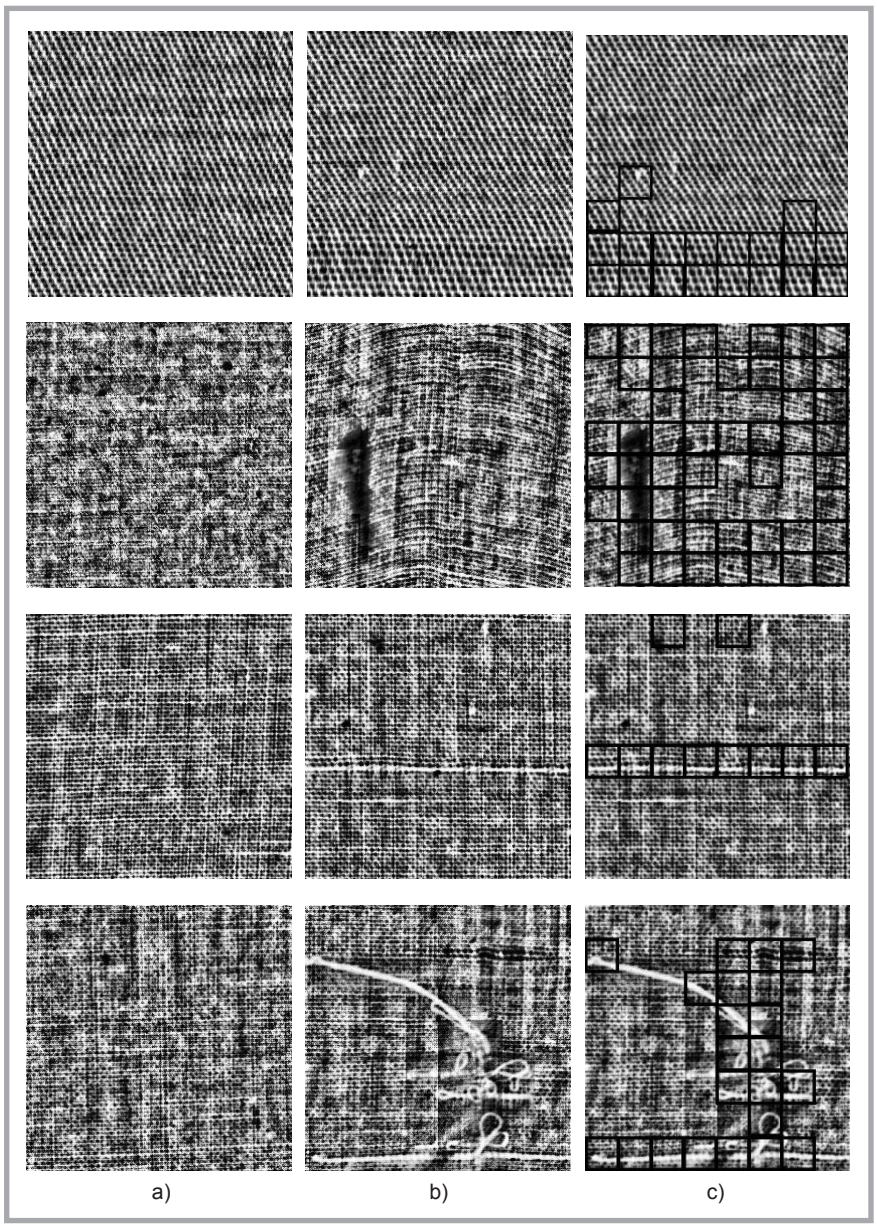


***Figure 6.*** *Figurative examples of detection results: a) normal fabric images, b) defective fabric images, c) detection results.*


## Acknowledgements

*The authors would like to thank the National Natural Science Foundation of China [61501209, 61379011], the Postdoctoral Project [1601017A] and a project funded by the Priority Academic Program Development of Jiangsu Higher Education Institutions (PAPD).*


## References


1. Ngan HYT, Pang GKH, Yung NHC. Automated fabric defect detection a review. *Image and Vision Computing* 2011; 7: 442-458.
2. Cohen F, Fan Z, Attali S. Automated inspection of textile fabrics using textural models. *Pattern Analysis and Machine Intelligence* 1991; 8: 803-808.
3. Baykut A, Atalay A, Erçil A, Güler M. Real-time defect inspection of textured surfaces. *Real-Time Imaging* 2000; 1: 17-27.
4. Latif-Amet A, Ertüzün A, Erçil A. An efficient method for texture defect detection: sub-band domain co-occurrence matrices. *Image and Vision Computing* 2000; 6: 543-553.
5. Chan CH, Pang GKH. Fabric defect detection by Fourier analysis. *IEEE Transactions on Industry Applications* 1999; 5: 1743-1750.
6. Yang XZ, Pang G, Yung N. Discriminative training approaches to fabric defect classification based on wavelet transform. *Pattern Recognition* 2004; 5: 889-899.
7. Kim SC, Kang TJ. Texture classification and segmentation using wavelet packet frame and Gaussian mixture model. *Pattern Recognition* 2007; 4: 1207-1221.

8. Hou Z, Parker JM. Texture defect detection using support vector machines with adaptive gabor wavelet features. In: *7th IEEE Workshop on Applications of Computer Vision*, 2005; pp. 275-280, New Jersey: IEEE.
9. Pentland AP. Fractal-based description of natural scenes. *Pattern Analysis and Machine Intelligence* 1984; 6: 661-674.
10. Lundahl T, Ohley WJ, Kay SM, Siffert R. Fractal Brownian motion: A maximum likelihood estimator and its application to image texture. *IEEE Transactions on Medical Imaging* 1986; 3: 152-161.
11. Chen CC, Daponee JS, Fox M D. Fractal feature analysis and classification in medical imaging. *Transactions on Medical Imaging* 1989; 2: 133-142.
12. Conci A, Proença CB. Fractal image analysis system for fabric inspection based on a box-counting method. *Computer Networks and ISDN Systems* 1998; 20: 1887-1895.
13. Wen CY, Chou S, Liaw JJ. Textural defect segmentation using a fourier-domain maximum likelihood estimation method. *Textile Research Journal* 2002; 3: 253-258.
14. Bu H, Huang X. A novel multiple fractal features extraction framework and its application to the detection of fabric defects. *Journal of the Textile Institute* 2013; 5: 489-497.
15. Parrinello T, Vaughan RA. Multifractal Analysis and feature extraction in satellite imagery. I*nternational Journal of remote sensing* 2002; 9: 1799-1825.
16. Lassouaoui N, Belouchrani A, Hamami-Mitiche L. On the use of multifractal analysis and genetic algorithms for the segmentation of cervical cell images. *International Journal of Pattern Recognition and Artificial Intelligence* 2003; 7: 1227-1244.
17. Bezdek JC, *Pattern Recognition with Fuzzy Objective Function Algorithms*. New York: Plenum, 1981.
18. Balafar MA, Ramli R, Iqbal SM, Mahmud R, Mashohor S, Balafar H. MRI segmentation of Medical images using FCM with initialized class centers via genetic algorithm. *International Symposium on Information Technology.* Kuala Lumpur, Malaysia, 2008, pp. 1-4.
19. Lee DJ, Lee JP, Ji PS, Park JW, Lim JY. Fault Diagnosis of Power Transformer Using SVM and FCM. *Conference Record of the 2008 IEEE International Symposium on Electrical Insulation*, Vancouver, BC, 2008, pp. 112-115.
20. Pruess SA *Fractals in the earth sciences*. New York: Springer, 1994.
21. Gao XB. *Fuzzy clustering analysis and application*. Xian: Xi Dian Press, 2004.
22. Pal NR, Bezdek JC On Clustering for the fuzzy c-means model. *IEEE Transactions on Fuzzy System* 1995; 3: 370-379.

***Received 29.11.2016 Reviewed 23.08.2017***